Evidence for [2Fe-2S] 2+ and Linear [3Fe-4S] 1+ Clusters in a Unique Family of Glycine/Cysteine-Rich Fe-S Proteins from Megavirinae Giant Viruses

Alejandro Villalta, Batoul Srour, Audrey Lartigue, Martin Clémancey, Deborah Byrne, Florence Chaspoul, Antoine Loquet, Bruno Guigliarelli, Geneviève Blondin, Chantal Abergel, et al.

Evidence for $[2Fe\text{-}2S]^{2+}$ and linear $[3Fe\text{-}4S]^{1+}$ clusters in a unique family of glycine/cysteine-rich Fe-S proteins from *Megavirinae* giant viruses

Alejandro Villalta[1‡], Batoul Srour[2‡], Audrey Lartigue[1], Martin Clémancey[3], Deborah Byrne[4], Florence Chaspoul[5], Antoine Loquet[6], Bruno Guigliarelli[2], Geneviève Blondin[3], Chantal Abergel[1*], Bénédicte Burlat[2*]

[1] Aix-Marseille Univ, CNRS, Information Génomique et Structurale (IGS), IMM FR3479, IM2B, IOM, Marseille, 13288, France

[2] Aix-Marseille Univ, CNRS, Bioénergétique et Ingénierie des Protéines (BIP), IMM FR3479, IM2B, Marseille, 13402, France

[3] Univ Grenoble Alpes, CNRS, CEA, Laboratoire de Chimie et Biologie des Métaux (LCBM), Grenoble, 38000, France

[4] Aix-Marseille Univ, CNRS, Expression Facility, Institut de Microbiologie de la Méditerranée (IMM), Marseille, 13402, France

[5] Aix Marseille Univ, Avignon Université, CNRS, IRD, Institut Méditerranéen de la Biodiversité et d'Ecologie marine et continentale (IMBE), Marseille, 13005, France

[6] Univ of Bordeaux, CNRS, IECB, CBMN, Pessac, 33600, France

‡ These authors equally contribute.

Supporting Information Placeholder

ABSTRACT: We have discovered a protein with an amino acid composition exceptionally rich in glycine and cysteine residues in the giant virus mimivirus. This small 6 kDa protein is among the most abundant proteins in the icosahedral 0.75 μm viral particles, it has no predicted function but is probably essential for infection. The aerobically purified red-brownish protein overproduced in *Escherichia coli* contained both iron and inorganic sulfide. UV/vis, EPR, and Mössbauer studies revealed that the viral protein, coined GciS, accommodated two distinct Fe-S clusters: a diamagnetic S=0 $[2Fe\text{-}2S]^{2+}$ cluster and a paramagnetic S=5/2 linear $[3Fe\text{-}4S]^{1+}$ cluster, a geometry rarely stabilized in native proteins. Orthologs of mimivirus GciS were identified within all clades of *Megavirinae*, a *Mimiviridae* subfamily infecting *Acanthamoeba*, including the distantly related tupanviruses, and displayed the same spectroscopic features. Thus, these glycine/cysteine-rich proteins form a new family of viral Fe-S proteins sharing unique Fe-S cluster binding properties.

Iron-sulfur (Fe-S) clusters are inorganic cofactors of proteins made of iron and sulfide and are essential for life.[1] Fe-S cluster-containing proteins are involved in many biological functions including redox and nonredox catalysis, sensing, gene expression, and regulation.[2-5] The most common Fe-S structural arrangements found in proteins are [2Fe-2S], cubane [4Fe-4S], and to a lesser extent, cubane [3Fe-4S] clusters.[6] Unusual Fe-S cluster architectures are also encountered in proteins for specific biological purposes.[2] Many Fe-S cluster mimics have been synthesized, providing a library of complex models with a large compositional and structural diversity.[7] Interestingly, synthetic models of $[3Fe\text{-}4S]^{1+}$ clusters with thiolate ligands exist only as a linear 3Fe-arrangement, whereas protein structural constraints promote the $[3Fe\text{-}4S]^{1+}$ cuboidal geometry.[7-8] Here we report on a new family of viral proteins, discovered in giant viruses, that bind Fe-S clusters, different from the few other viral Fe-S proteins characterized so far.[9-13] The recombinant GciS (Glycine/Cysteine-rich Iron-Sulfur) protein displays unique Fe-S binding properties, hence spontaneously stabilizing a linear-type $[3Fe\text{-}4S]^{1+}$ cluster together with a $[2Fe\text{-}2S]^{2+}$ cluster. These structural features may be clues to discovering novel functions for viral Fe-S proteins during infection.

Giant viruses are nucleocytoplasmic large DNA viruses (NCLDVs)[14] with up to 2.8 Mb genomes encoding 1500 proteins, most of them without resemblance to other cellular or viral proteins (ORFans).[15-16] Giant viruses are found in diverse habitats and infect eukaryotes, mostly protists and microalgae (reviewed in[17]). The first giant virus, mimivirus, was discovered in 2003. It has a 1.2 Mb genome encased in icosahedral capsids of ~0.75 μm diameter, visible by light microscopy, and replicates in the amoeba of the *Acanthamoeba* genus.[18-19] Transcriptomic analysis of *Acanthamoeba castellanii* infected by mimivirus revealed a small gene with no-predicted function, *R633b*, the one that is the most transcribed during the late phase of infection.[20] Mass spectrometry-based proteomics confirmed that *R633b* encodes a 59-amino acid protein peculiarly rich in glycine, cysteine, and aromatic residues (**Fig. 1**). This low-complexity protein is among the most abundant in the viral particles.

MS**C**FGGWNGG**C**GP**C**GGFGWGG**C**GPSWG**C**GP**C**GFGGGY-SYRVSYGFGG**C**GFPGGFGWGG**CC**

Figure 1. Amino acid sequence of GciS mimivirus encoded by the R633b gene.

Expression of the *R633b* gene in *Escherichia coli* (*Ec*) grown aerobically led to red-colored cell pellets (**Fig S1**). The

corresponding air-purified protein expressed in fusion with a His_6-SUMO tag was most soluble at extreme *pH* values (4 or 10.5), showed a red brownish color, and formed large oligomers, as seen by size-exclusion chromatography and transmission electron microscopy (**Figs S1 and S2**). Metal content analysis by Inductively Coupled Plasma-Mass Spectrometry (ICP-MS) indicated that the recombinant protein contained only iron. Furthermore, ICP-MS and chemical analysis returned iron and acid-labile sulfide contents of 0.65 (± 0.10) and 0.70 (± 0.20) per protein respectively, giving a Fe to S^{2-} ratio of 0.9 ± 0.3 consistent with the presence of a Fe-S cluster.

The optical spectrum of the air-purified protein at *pH* 10.5 displayed a broad absorption in the near-UV and visible regions, with several absorbance bands at 335, 418, 462, 513, and 586 nm characteristics of sulfur-to-iron charge transfer bands (**Fig. 2a**). This optical spectrum was different from those observed for cubane $[4Fe\text{-}4S]^{2+}$ or $[3Fe\text{-}4S]^{1+}$ clusters, but reminiscent of $[2Fe\text{-}2S]^{2+}$ centers (330, 420, 460, and 550 nm).[21-22] Features near 600 nm are less common and more characteristics of linear-type $[3Fe\text{-}4S]^{1+}$ clusters.[22-24] Taking into account the extinction coefficients of $\varepsilon_{420nm} \sim 10$ mM^{-1} cm^{-1} and $\varepsilon_{280nm} \sim 15$ mM^{-1} cm^{-1} for synthetic $[2Fe\text{-}2S]^{2+}$ clusters[22], and $\varepsilon_{280nm} \sim 30$ mM^{-1} cm^{-1} for the GciS polypeptide chain, the presence of one $[2Fe\text{-}2S]^{2+}$ cluster per monomer would lead to a A_{420nm}/A_{280nm} ratio value of 10/45 = 0.22. Using various GciS preparations from mimivirus, we determined a A_{420nm}/A_{280nm} ratio of 0.12 ± 0.02 (**Fig. 2a**) which gives a crude estimation of 0.12/0.22 = 0.54 Fe-S cluster per monomer in agreement with iron and sulfide contents. Similar spectra were obtained at *pH* 4 and 7.8 (**Fig. S3**). Finally, the protein isolated anaerobically from bacterial cells grown aerobically gave an optical spectrum identical to that of the protein purified aerobically and was unchanged upon exposure to air (**Fig. S4**). This showed that the nature and content of Fe-S clusters are insensitive to O_2 during protein purification or afterward.

The X-band EPR spectrum of the mimivirus air-purified GciS protein recorded at 15 K displayed only a sharp resonance at $g \sim 4.3$ and a broad absorption feature at $g \sim 9.1$ characteristics of a rhombic S=5/2 system (**Fig. 2b**). The resonance line at $g \sim 9.1$ originates from the lowest and upper Kramers doublets, and the $g \sim 4.3$ resonance line from the middle Kramers doublet. The minimum observed at $g \sim 4.15$ was consistent with a zero-field splitting (ZFS) rhombicity E/D of 0.27, close to the maximum value (1/3). A minor contribution of adventitious ferric iron was also detected at $g \sim 4.27$ (asterisks in **Figs 2b, 4**). The total S=5/2 species accounted for 0.10 ± 0.03 spin per protein. In nonheme iron-containing proteins, S=5/2 species can correspond either to a mononuclear ferric iron species, such as in rubredoxin,[25] or a linear $[3Fe\text{-}4S]^{1+}$ cluster.[23] The temperature dependence study of the $g \sim 4.3$ signal between 3.6 and 40 K gave a ZFS axial parameter (D) of 0.6 ± 0.2 cm^{-1} (**Fig. S5**). This value was similar to those determined for the linear $[3Fe\text{-}4S]^{1+}$ cluster in synthetic model (D = 0.7 ± 0.2 cm^{-1}), purple aconitase (D = 1.5 ± 0.2 cm^{-1}) and *Saccharomyces cerevisiae* (*Sc*) monothiol glutaredoxin (Grx5) (0.6 ± 0.2 cm^{-1}).[24, 26] Furthermore, the broadness and asymmetry of the $g \sim 9.1$ peak indicated large D-strain for the S=5/2 species, reflecting conformational distribution of the protein.[27] Overall, this S=5/2 species was consistent with a linear $[3Fe\text{-}4S]^{1+}$ cluster by comparison with previous spectroscopic characterizations of linear $[3Fe\text{-}4S]^{1+}$ clusters.[23-24] This $g \sim 4.3$ signal was also visible in purified samples solubilized at *pH* 4 or 7.8 (**Fig. S3**), in whole *Ec* cells overproducing mimivirus GciS without the SUMO tag, as well as in the purified mimivirus particles (**Fig. 3**). The S=5/2 species is therefore independent of the *pH*, SUMO tag, aerobic purification process, and biosynthesis by the bacterial or amoebal Fe-S cluster assembly machinery. In other words, the S=5/2 linear $[3Fe\text{-}4S]^{1+}$ is an inherent feature of the viral protein.

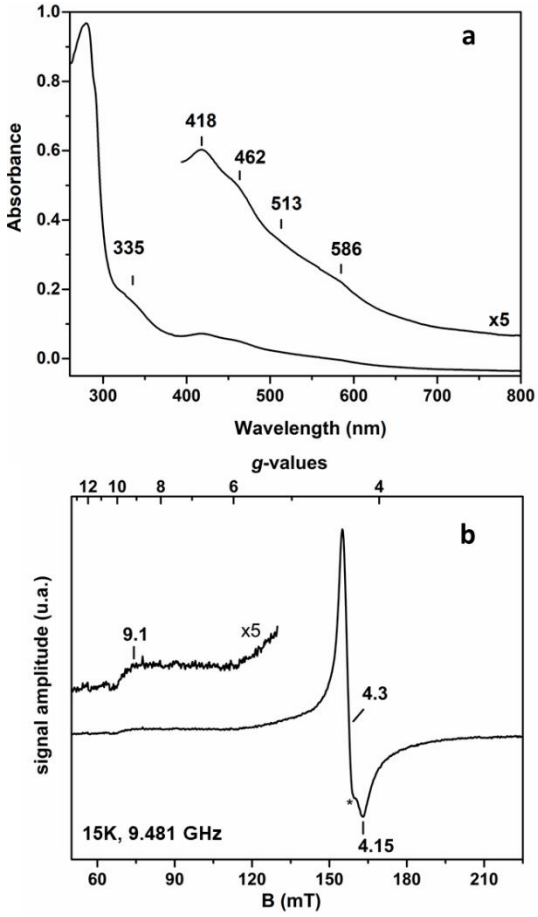

*Figure 2. (**a**) UV/vis and (**b**) EPR signatures of the Fe-S cluster in mimivirus recombinant tagged GciS protein purified aerobically and solubilized at pH 10.5.*

To further characterize the Fe-S clusters in GciS and confirm the presence of a linear $[3Fe\text{-}4S]^{1+}$ species, Mössbauer experiments were performed on isotopically ^{57}Fe enriched purified GciS samples at high concentration (7 mM in protein). **Fig. 4** reproduces the Mössbauer spectra recorded at *ca* 6 K using an external magnetic field ranging from 0.06 to 7 T applied parallel to the γ-rays. The 60 mT spectrum presents an intense doublet that is characteristic of diamagnetic $[2Fe\text{-}2S]^{2+}$ clusters.[28] This was indeed confirmed by the two spectra recorded using higher magnetic fields. More importantly, the 4 and 7 T spectra revealed another broad contribution that extends from –5 to +5 mm s^{-1}. The lines detected on both edges of the diamagnetic $[2Fe\text{-}2S]^{2+}$ cluster contribution are strongly reminiscent of those observed for linear $[3Fe\text{-}4S]^{1+}$ clusters.[25,26] The three spectra recorded at various magnetic fields can be well reproduced by considering the contributions of two all-ferric clusters, the S=0 ground state of the $[2Fe\text{-}2S]^{2+}$ cluster on one hand, and the S=5/2 ground state of the linear $[3Fe\text{-}4S]^{1+}$ cluster on the other hand (**Fig. 4**).

Table 1. Mössbauer parameters used to reproduce spectra shown in Fig. 4 and Fig. S6[a]

Fe site	$A_i/(g_n\mu_n)$ (i=x,y,z)/ (T)[b]			δ (mm.s^{-1})	ΔE_Q (mm.s^{-1})	η	Relative area (%)
	x	*y*	*z*				
S=5/2 [3Fe-4S]$^{1+}$ (assuming D = 0.6 cm^{-1}, E/D = 0.27, $g_x = g_y = g_z$ = 2.0 from EPR studies)							
1	−11.7	−13.4	−11.7	0.28	−0.64	−1.2	9
2	−11.6	−14.3	−13.8	0.28	−0.73	−1.3	9
3	9.9	10.3	10.0	0.32	0.57	0.5	9
S=0 [2Fe-2S]$^{2+}$							
4	-	-	-	0.27	0.53	0.5	36
5	-	-	-	0.28	0.52	1.4	36

Because the 60 mT spectrum is lacking clearly resolved lines originating from the linear [3Fe-4S]$^{1+}$ cluster, quadrupole splitting values could not be accurately determined. Accordingly, those previously reported for the linear [3Fe-4S]$^{1+}$ cluster of *Sc* Grx5 reconstituted in the presence of glutathione were used.[24] The ZFS parameters were fixed to the values determined from the EPR studies, namely D = 0.6 cm^{-1} and E/D = 0.27. The hyperfine coupling constants obtained here were perfectly consistent with a linear [3Fe-4S]$^{1+}$ cluster where the central high-spin ferric ion (Site 3) is antiferromagnetically coupled with the two-terminal high-spin ferric ions (Sites 1 and 2), leading to an *S*=5/2 ground state (**Fig. S6**). The parameters used to reproduce the Mössbauer spectra are listed in **Table 1**. According to the contributions indicated in **Table 1** and the total iron content of 0.65 Fe per protein determined by ICP-MS, this gave 0.23 [2Fe-2S]$^{2+}$ and 0.06 [3Fe-4S]$^{1+}$ clusters per protein monomer. Within the uncertainties, this is overall consistent with the Fe-S clusters content estimated from EPR and UV/vis analyses.

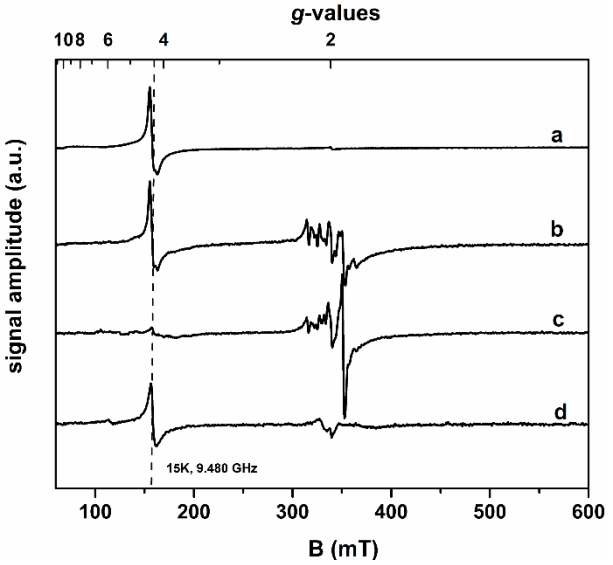

Figure 3 X-band EPR spectra of mimivirus recombinant tagged GciS purified aerobically at pH=10.5 ***(a)****, whole Ec cells overproducing mimivirus GciS (R633b gene)* ***(b)*** *or another gene (R341) as a negative control* ***(c)****, and purified mimivirus particles* ***(d)****.*

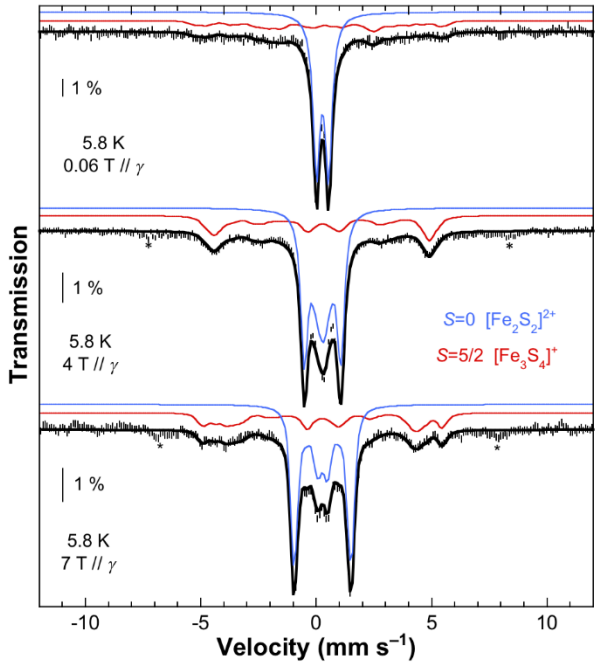

Figure 4. Mössbauer spectra of mimivirus air-purified recombinant GciS showing the signatures of (S=0) [2Fe-2S]$^{2+}$ and (S=5/2) linear [3Fe-4S]$^{1+}$ clusters. The black line is the spectral simulation resulting from the addition of individual cluster contributions.

Finally, we aimed to determine whether GciS was conserved within *Megavirinae,* a proposed subfamily of *Mimiviridae.*[17] A simple blast search without filtering revealed that the protein was conserved in all members of clade A (mimivirus). Bioinformatic analyses also showed that orthologues of GciS from mimivirus may be found in other members of the subfamily. Possible orthologues were identified in clades B (moumouviruses), C (megaviruses) and D (tupanviruses). Despite sequence variability between clades, all display high glycine, cysteine, and aromatic residue contents (**Fig S7**). All air-purified recombinant proteins from mimivirus, moumouvirus, moumouvirus australiensis, moumouvirus maliensis, megavirus chilensis and tupanvirus soda lake were brownish red and contained less than 0.9 iron per monomer (**Table S1**). As for mimivirus, the purified proteins displayed similar UV/vis and EPR spectra reflecting the presence of both [2Fe-2S]$^{2+}$ and linear [3Fe-4S]$^{1+}$ clusters (**Fig. 5**). We estimated that the *S*=5/2 linear [3Fe-4S]$^{1+}$ cluster accounted for between 0.03 and 0.10 cluster per protein, and the [2Fe-2S]$^{2+}$ cluster accounted for between 0.04 and 0.30 cluster per protein (**Table S1**). In summary, this shows that these sequences retrieved by bioinformatic analysis define a new family of proteins, featuring small sizes, with low-

complexity glycine, cysteine and aromatic-rich sequences, and with the innate ability to stabilize Fe-S clusters in the form of [2Fe-2S]$^{2+}$ and linear [3Fe-4S]$^{1+}$ clusters. In addition, ongoing studies of the dithionite-reduced proteins by Mössbauer and EPR reveal that both Fe-S clusters cannot redox cycle.

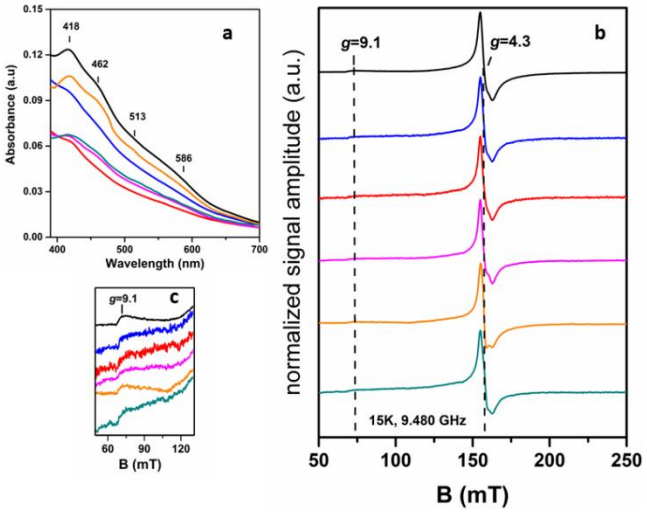

*Figure 5. UV/vis (**a**) and EPR signatures (**b, c:** zoom around 90 mT) of GciS proteins from clades A (mimivirus, black), B (moumouvirus, moumouvirus australiensis, and moumouvirus maliensis in blue, red, and pink, respectively), C (megavirus chilensis, orange), and D (tupanvirus soda lake, green).*

In conclusion, we identified a linear-type [3Fe-4S]$^{1+}$ cluster as well as a [2Fe-2S]$^{2+}$ cluster in the small, low-complexity, Fe-S proteins from *Megavirinae* giant viruses. These Fe-S clusters were observed independently from *pH* and the presence of O_2 during (or after) protein purification. Viral particles of *Megavirinae* contain a wealth of these Fe-S proteins which raises questions about their role during host/virus interaction. Indeed, the linear 3Fe arrangement was barely observed in proteins and was never associated with any known physiological function. This unusual geometry in biology was first revealed in synthetic Fe-S models in the early 1980s,[22, 29-30] before being identified in oxidized and partially unfolded mitochondrial beef-heart aconitase.[23] The linear 3Fe form was also detected in a few [4Fe-4S]-containing enzymes[31-34] and unfolded ferredoxins,[35-38] and was most often attributed to a degraded Fe-S form. More recently, stabilization in the presence of glutathione of a linear [3Fe-4S]$^{1+}$ cluster in *Sc* Grx5, an important component in Fe-S cluster biogenesis, led to the proposal that the linear 3Fe form may be an intermediate during Fe-S cluster assembly.[24] Investigating the Fe-S binding properties of GciS proteins, in the context of their structural properties, is thus an essential prerequisite to give clues to their physiological role and perhaps unveil new functions for viral Fe-S proteins.

ASSOCIATED CONTENT

Supporting Information

Figures and data supplied as Supporting Information (PDF): Pictures of GciS in bacterial pellets and purified sample (**Fig S1**); Size-exclusion chromatography and negative staining transmission electron microscopy images of mimivirus GciS (**Fig S2)**; Optical and EPR spectra of mimivirus recombinant tagged GciS purified aerobically and solubilized at *pH* 4 and 7.8 (**Fig S3)**. Optical and X-band EPR spectra of megavirus recombinant tagged GciS purified anaerobically and after exposure to air (**Fig S4)**. Determination of *D* parameter from EPR experiments (**Fig. S5**); Mössbauer subspectra of the linear ground state *S*=5/2 [3Fe-4S]$^{1+}$ cluster (**Fig. S6**); GciS protein sequences of each viral clade prototype (**Fig. S7**); Estimation of iron and Fe-S contents in recombinant air-purified tagged GciS proteins from *Megavirinae* clades A to D (**Table S1**).
Materials and methods, including protein purification, and experimental conditions for spectroscopy (PDF). The Supporting Information is available free of charge on the ACS Publications website.

AUTHOR INFORMATION

Corresponding Author

Correspondence should be addressed to Bénédicte Burlat, bburlat@imm.cnrs.fr or Chantal Abergel, abergel@igs.cnrs-mrs.fr.

Author Contributions

‡These authors contributed equally.

Notes

The authors declare no competing financial interests.

ACKNOWLEDGMENT

This work was funded by the French national research agency (ANR-16-CE11-0033 VIRiON) and received funding from the European Research Council (ERC) under the European Union's Horizon 2020 research and innovation program (grant agreement No 832601, granted to CA). MC and GB acknowledge the French National Research Agency (Labex ARCANE, CBH-EUR-GS, ANR-17-EURE-0003). The authors thank the EPR-MRS facility of the French Research Infrastructure INFRANALYTICS (FR2054) and the Aix-Marseille University EPR center. The authors thank Dr. B. Faure for the ^{57}Fe-Mohr's salt synthesis and Dr. S. Ollagnier for protocols for acid-labile sulfide and iron contents determination. Preliminary electron microscopy experiments were performed on the IMM imaging platform (A. Kosta) and PiCSL-FBI core facility (N. Brouilly, F. Richard and A. Aouane, IBDM, AMU-Marseille), member of the France -BioImaging national research infrastructure.

REFERENCES AND FOOTNOTES

Footnotes

[a] Contributions of sites 1–3 were assumed to be equal, as those of sites 4 and 5.

[b] Uncertainties on the x- and z-components are estimated to 1 T and those on the y-components to 0.4 T.

References

1. Beinert, H.; Holm, R. H.; Munck, E., Iron-sulfur clusters: Nature's modular, multipurpose structures. *Science* **1997,** *277* (5326), 653-659.
2. Beinert, H., Iron-sulfur proteins: ancient structures, still full of surprises. *J. Biol. Inorg. Chem.* **2000,** *5* (1), 2-15.
3. Fontecave, M., Iron-sulfur clusters: ever-expanding roles. *Nat. Chem. Biol.* **2006,** *2* (4), 171-174.
4. Mettert, E. L.; Kiley, P. J., Fe-S proteins that regulate gene expression. *Biochim. Biophys. Acta* **2015,** *1853* (6), 1284-93.
5. Honarmand Ebrahimi, K.; Ciofi-Baffoni, S.; Hagedoorn, P.-L.; Nicolet, Y.; Le Brun, N. E.; Hagen, W. R.; Armstrong, F. A., Iron–sulfur clusters as inhibitors and catalysts of viral replication. *Nature Chemistry* **2022,** *14* (3), 253-266.
6. Guigliarelli, B.; Bertrand, P., Application of EPR spectroscopy to the structural and functional study of iron-sulfur proteins. In *Advances in*

Inorganic Chemistry, Vol 47: Iron-Sulfur Proteins, Sykes, A. G., Ed.; Academic Press Inc Elsevier Science, **1999**; pp 421-497.
7. Holm, R. H.; Lo, W., Structural Conversions of Synthetic and Protein-Bound Iron-Sulfur Clusters. *Chem. Rev.* **2016,** *116* (22), 13685-13713.
8. Beinert, H.; Kennedy, M. C., 19th Sir Hans Krebs lecture. Engineering of protein bound iron-sulfur clusters. A tool for the study of protein and cluster chemistry and mechanism of iron-sulfur enzymes. *Eur. J. Biochem.* **1989,** *186* (1-2), 5-15.
9. Martin, D.; Charpilienne, A.; Parent, A.; Boussac, A.; D'Autreaux, B.; Poupon, J.; Poncet, D., The rotavirus nonstructural protein NSP5 coordinates a [2Fe-2S] iron-sulfur cluster that modulates interaction to RNA. *FASEB J.* **2013,** *27* (3), 1074-83.
10. Tsang, S. H.; Wang, R.; Nakamaru-Ogiso, E.; Knight, S. A.; Buck, C. B.; You, J., The Oncogenic Small Tumor Antigen of Merkel Cell Polyomavirus Is an Iron-Sulfur Cluster Protein That Enhances Viral DNA Replication. *J. Virol.* **2016,** *90* (3), 1544-56.
11. Maio, N.; Lafont, B. A. P.; Sil, D.; Li, Y.; Bollinger, J. M., Jr.; Krebs, C.; Pierson, T. C.; Linehan, W. M.; Rouault, T. A., Fe-S cofactors in the SARS-CoV-2 RNA-dependent RNA polymerase are potential antiviral targets. *Science* **2021,** *373* (6551), 236-241.
12. Ueda, C.; Langton, M.; Chen, J.; Pandelia, M. E., The HBx protein from hepatitis B virus coordinates a redox-active Fe-S cluster. *J. Biol. Chem.* **2022,** *298* (4), 101698.
13. Tam, W.; Pell, L. G.; Bona, D.; Tsai, A.; Dai, X. X.; Edwards, A. M.; Hendrix, R. W.; Maxwell, K. L.; Davidson, A. R., Tail tip proteins related to bacteriophage λ gpL coordinate an iron-sulfur cluster. *J. Mol. Biol.* **2013,** *425* (14), 2450-62.
14. Iyer, L. M.; Aravind, L.; Koonin, E. V., Common origin of four diverse families of large eukaryotic DNA viruses. *J. Virol.* **2001,** *75* (23), 11720-34.
15. Abergel, C.; Legendre, M.; Claverie, J. M., The rapidly expanding universe of giant viruses: Mimivirus, Pandoravirus, Pithovirus and Mollivirus. *FEMS Microbiol. Rev.* **2015,** *39* (6), 779-96.
16. Schulz, F.; Abergel, C.; Woyke, T., Giant virus biology and diversity in the era of genome-resolved metagenomics. *Nat. Rev. Microbiol.* **2022,** *20* (12), 721-736.
17. Speciale, I.; Notaro, A.; Abergel, C.; Lanzetta, R.; Lowary, T. L.; Molinaro, A.; Tonetti, M.; Van Etten, J. L.; De Castro, C., The Astounding World of Glycans from Giant Viruses. *Chem. Rev.* **2022,** *122* (20), 15717-15766.
18. Raoult, D.; Audic, S.; Robert, C.; Abergel, C.; Renesto, P.; Ogata, H.; La Scola, B.; Suzan, M.; Claverie, J. M., The 1.2-megabase genome sequence of Mimivirus. *Science* **2004,** *306* (5700), 1344-50.
19. La Scola, B.; Audic, S.; Robert, C.; Jungang, L.; de Lamballerie, X.; Drancourt, M.; Birtles, R.; Claverie, J. M.; Raoult, D., A giant virus in amoebae. *Science* **2003,** *299* (5615), 2033.
20. Legendre, M.; Santini, S.; Rico, A.; Abergel, C.; Claverie, J. M., Breaking the 1000-gene barrier for Mimivirus using ultra-deep genome and transcriptome sequencing. *J. Virol.* **2011,** *8*, 99.
21. Dermoun, Z.; De Luca, G.; Asso, M.; Bertrand, P.; Guerlesquin, F.; Guigliarelli, B., The NADP-reducing hydrogenase from Desulfovibrio fructosovorans: functional interaction between the C-terminal region of HndA and the N-terminal region of HndD subunits. *Biochim. Biophys. Acta* **2002,** *1556* (2-3), 217-25.
22. Hagen, K. S.; Watson, A. D.; Holm, R. H., Synthetic routes to Fe_2S_2, FeS_4, Fe_4S_4, and Fe_6S_9 clusters from the common precursor $[Fe(SC_2H_5)_4]^{2-}$ - Structures and properties of $[Fe_3S_4(SR)_4]^{3-}$ and $[Fe_6S_9(SC_2H_5)_2]^{4-}$, examples of the newest types of Fe-S-SR clusters *J. Am. Chem. Soc.* **1983,** *105* (12), 3905-3913.
23. Kennedy, M. C.; Kent, T. A.; Emptage, M.; Merkle, H.; Beinert, H.; Munck, E., Evidence for the formation of a linear [3Fe-4S] cluster in partially unfolded aconitase. *J. Biol. Chem.* **1984,** *259* (23), 14463-71.
24. Zhang, B.; Bandyopadhyay, S.; Shakamuri, P.; Naik, S. G.; Huynh, B. H.; Couturier, J.; Rouhier, N.; Johnson, M. K., Monothiol glutaredoxins can bind linear $[Fe_3S_4]^+$ and $[Fe_4S_4]^{2+}$ clusters in addition to $[Fe_2S_2]^{2+}$ clusters: spectroscopic characterization and functional implications. *J. Am. Chem. Soc.* **2013,** *135* (40), 15153-64.
25. Peisach, J.; Blumberg, W. E.; Lode, E. T.; Coon, M. J., An analysis of the electron paramagnetic resonance spectrum of pseudomonas oleovorans rubredoxin. A method for determination of the liganids of ferric iron in completely rhombic sites. *J. Biol. Chem.* **1971,** *246* (19), 5877-81.
26. Richards, A. J. M.; Thomson, A. J.; Holm, R. H.; Hagen, K. S., The magnetic circular dichroism spectra of the linear trinuclear clusters $[Fe_3S_4(SR)_4]^{3-}$ in purple aconitase and in a synthetic model. *Spectrochim Acta A* **1990,** *46* (6), 987-993.
27. Hagen, W. R., *Biomolecular EPR spectroscopy*; CRC Press, Taylor & Francis Group, Boca Raton, **2009**.
28. Pandelia, M. E.; Lanz, N. D.; Booker, S. J.; Krebs, C., Mossbauer spectroscopy of Fe/S proteins. *Biochim. Biophys. Acta - Mol Cell Res* **2015,** *1853* (6), 1395-1405.
29. Hagen, K. S.; Holm, R. H., Systematic iron(II)-thiolate chemistry - synthetic entry to trinuclear complexes. *J. Am. Chem. Soc.* **1982,** *104* (20), 5496-5497.
30. Girerd, J. J.; Papaefthymiou, G. C.; Watson, A. D.; Gamp, E.; Hagen, K. S.; Edelstein, N.; Frankel, R. B.; Holm, R. H., Electronic properties of the linear antiferromagnetically coupled clusters $[Fe_3S_4(SR)_4]^{3-}$, structural isomers of $[Fe_3S_4]^+$ unit in iron sulfur proteins. *J. Am. Chem. Soc.* **1984,** *106* (20), 5941-5947.
31. Gailer, J.; George, G. N.; Pickering, I. J.; Prince, R. C.; Kohlhepp, P.; Zhang, D.; Walker, F. A.; Winzerling, J. J., Human cytosolic iron regulatory protein 1 contains a linear iron-sulfur cluster. *J. Am. Chem. Soc.* **2001,** *123* (41), 10121-2.
32. Flint, D. H.; Emptage, M. H.; Finnegan, M. G.; Fu, W.; Johnson, M. K., The role and properties of the iron-sulfur cluster in Escherichia coli dihydroxy-acid dehydratase. *J. Biol. Chem.* **1993,** *268* (20), 14732-42.
33. Krebs, C.; Broderick, W. E.; Henshaw, T. F.; Broderick, J. B.; Huynh, B. H., Coordination of adenosylmethionine to a unique iron site of the [4Fe-4S] of pyruvate formate-lyase activating enzyme: a Mössbauer spectroscopic study. *J. Am. Chem. Soc.* **2002,** *124* (6), 912-3.
34. Liu, A.; Gräslund, A., Electron paramagnetic resonance evidence for a novel interconversion of $[3Fe\text{-}4S]^+$ and $[4Fe\text{-}4S]^+$ clusters with endogenous iron and sulfide in anaerobic ribonucleotide reductase activase *in vitro*. *J. Biol. Chem.* **2000,** *275* (17), 12367-73.
35. Wittung-Stafshede, P.; Gomes, C. M.; Teixeira, M., Stability and folding of the ferredoxin from the hyperthermophilic archaeon Acidianus ambivalens. *J. Inorg. Biochem.* **2000,** *78* (1), 35-41.
36. Moczygemba, C.; Guidry, J.; Jones, K. L.; Gomes, C. M.; Teixeira, M.; Wittung-Stafshede, P., High stability of a ferredoxin from the hyperthermophilic archaeon A. ambivalens: involvement of electrostatic interactions and cofactors. *Protein Sci.* **2001,** *10* (8), 1539-48.
37. Jones, K.; Gomes, C. M.; Huber, H.; Teixeira, M.; Wittung-Stafshede, P., Formation of a linear [3Fe-4S] cluster in a seven-iron ferredoxin triggered by polypeptide unfolding. *J. Biol. Inorg. Chem.* **2002,** *7* (4-5), 357-62.
38. Higgins, C. L.; Wittung-Stafshede, P., Formation of linear three-iron clusters in Aquifex aeolicus two-iron ferredoxins: effect of protein-unfolding speed. *Arch. Biochem. Biophys.* **2004,** *427* (2), 154-63.

Table of Contents artwork